Study on the mechanism of anti-MIRI action of total flavones of Fructus Chorspondiatis by PET/CT imaging

Guo-Jian Zhang[1,2], Li-Hong Wei[3], Hai-Wen Lu[4], Yun-Feng Xiao[5], Wen-Rui Wang[2], Yu-Lin He[2], Xue-Mei Wang[2], Jia-He Tian[1]

[1]Medical School of Chinese PLA, Beijing, China; [2]Department of Nuclear Medicine, the Affiliated Hospital of Inner Mongolia Medical University, Hohhot, China; [3]Department of Pharmacy, Inner Mongolia International Mongolian Hospital, Hohhot, China; [4]Department of Imaging, the Affiliated Hospital of Inner Mongolia Medical University, Hohhot, China; [5]Center for New Drug Safety Evaluation and Research, Inner Mongolia Medical University, Hohhot, China

Contributions: (I) Conception and design: GJ Zhang, JH Tian; (II) Administrative support: HW Lu, XM Wang; (III) Provision of study material or animals: All authors; (IV) Collection and assembly of data: GJ Zhang, LH Wei; (V) Data analysis and interpretation: GJ Zhang, YF Xiao; (VI) Manuscript writing: All authors; (VII) Final approval of manuscript: All authors.

Correspondence to: Jia-He Tian, PhD. Department of Nuclear Medicine, Medical School of Chinese PLA, No.28 Fuxing Road, Haidian District, Beijing, 100853 China. Email: bj_tianjiahe@163.com.

Background: To investigate anti myocardial ischemia/reperfusion injury (MIRI) action of total flavones of Fructus Chorspondiatis (TFFC) in rats by ^{13}N-ammonia micro PET/CT imaging, etc.

Methods: Male Sprague-Dawley rats were randomly divided into 6 groups. Micro PET/CT imaging was performed before and after modeling to calculate the volume (VOI) and SUV$_{mean}$ of myocardial ischemic area. The oxidative stress index [(superoxide dismutase (SOD), malondialdehyde (MDA)] and the marker enzymes [creatine kinase (CK), lactate dehydrogenase (LDH)] of myocardial injury were detected. The pathological changes of myocardial were observed via HE staining. A MIRI model of rat cardiomyocytes in vitro was established, the damage and apoptosis of myocardial cells in each group were observed, and the apoptosis rate of cardiomyocytes was detected.

Results: The imaging viscosities of the imaging agents were observed at 24 and 48 h in each group. The VOI of 24 h imaging was (6.33±2.02), (6.01±1.56) and (3.32±0.86) mm^3, respectively. The VOI of 48 h imaging was (3.31±1.33), (2.61±1.01) and (1.32±0.58) mm^3. The 72 h imaging medium and high dose group recovered, while the low dose group still saw sparseness with (1.26±0.68) mm^3 VOI. The ischemic (SUV$_{mean}$) gradually increased with time. Metabolism gradually recovered (F=121.82, 450.82, 435.75, P<0.05). The three doses of TFFC can eliminate free radicals and reduce the damage of myocardial injury. Amongst them, the high-dose group had a better effect on SOD, and the middle-dose group had a better effect on MDA and LDH. The low-dose group affected CK, and a significant difference was observed compared with the control group (P<0.05). After administration, the morphology of myocardial cells in each dose group was improved to some extent. Nuclear pyknosis, rupture, the apoptosis rate, etc. were significantly reduced, the number of cells increased. The high dose group showed the most obvious improvement.

Conclusions: The PET/CT imaging method can detect non-invasive, in vivo and dynamic MIRI, and can accurately evaluate the protective effect of traditional Mongolian medicine TFFC on MIRI. The Anti-MIRI of TFFC can scavenge free radicals, reduce oxidative stress damage, inhibit apoptosis, affect the activity of related enzymes.

Keywords: Total flavones of Fructus Chorspondiatis (TFFC); myocardial ischemia/reperfusion injury (MIRI); position emission tomography/computed tomography (PET/CT)

Introduction

Cardiovascular disorders, ranking the first in terms of incidence and mortality among all diseases including tumors, are the leading cause of death that threatens human health worldwide. According to the statistical data of the World Health Organization, approximately 17.5 million deaths are caused by heart diseases worldwide every year, thereby accounting for 30% of the total deaths. The incidence rate of cardiovascular disorders increases each year. To date, A total of 290 million patients with cardiovascular disorders are found in China (1). Developed economies have made remarkable progress in the prevention and treatment of cardiovascular disorders, while the development tendency of such diseases in developing countries is not optimistic. The mechanism underlying the decrease in incidence and mortality of heart diseases by effective interventions has become an increasingly urgent major public health issue. The survival rate of myocardial infraction has been considerably improved by the current treatment and prevention strategies. With the continuous development of ischemic myocardium reperfusion techniques, for instance, the establishment and promotion of coronary artery bypass grafting, thrombolytic therapy, percutaneous coronary intervention, and other methods, can achieve reperfusion following myocardial ischemia (2). However, reperfusion after myocardial ischemia would not help recover cardiac functions and even aggravate cardiac dysfunction and structural impairment (3), namely, myocardial ischemia/reperfusion injury (MIRI). MIRI is the key to restrict the therapeutic effect of ischemic myocardium reperfusion. The mechanism underlying MIRI alleviation and injured myocardium protection has always been an important problem of interest in clinical practice. Ethnic medicine has been intensively studied by many researchers and has achieved good curative effects in clinical application due to its advantages, such as natural sources, proven curative effect, and slight side effects. In clinical practice, early intervention to reduce myocardial injury caused by ischemia reperfusion contributes to the effect of reperfusion therapy (4).

Fructus Choerospondiatis is a Mongolian medicine which is frequently used in clinical treatment by Mongolian medicine. It has obvious effects in treating coronary heart disease, angina pectoris, antiarrhythmia, myocardial protection and other aspects, and has little side effect. It has been affirmed by basic research and clinical practice (5,6), but its mechanism of action has not been fully clarified.

The main active ingredient of Fructus Choerospondiatis is TFFC (7,8), which has been reported in research (9,10). TFFC can promote the anti-anoxia ability of myocardium, has obvious protective effect on ischemic myocardium and arrhythmia caused by myocardial ischemia, and can change hemorheology and hemodynamics, play the role of inhibiting platelet aggregation, scavenging free radicals and antioxidation, enhancing cellular immunity and humoral immune function, etc. We applied PET/CT imaging technology and combined with other detection methods to explore the mechanism of TFFC on MIRI, providing a theoretical basis for TFFC to treat MIRI, and also providing a noninvasive *in vivo* imaging evaluation method and research ideas for the future research and development of traditional Mongolian medicine.

We present the following article in accordance with the ARRIVE reporting checklist (available at http://dx.doi.org/10.21037/cdt-20-305).

Methods

In vivo MIRI rat model investigation

Experimental animals and grouping

One-hundred and twenty male SD rats of clean grade (bodyweight, 285±50 g) were purchased from the Animal Experimental Center of Inner Mongolia Medical University (number of animal license: SCXK 2016-0001). These animals were randomly divided into six 6 groups, with 20 animals in each group, as follows. Blank control group: The rats were gavaged with 0.5% CMC-Na (5 mL/kg/day) for 14 consecutive days. Model control group: The left anterior descending coronary artery (LAD) was ligated for 1 min, and reperfusion was performed after resuming the blood stream, and the sample was gavaged with 0.5% CMC-Na (5 mL/kg/day) for 14 straight days. The low-dose, medium-dose, and high-dose TFFC(National Mongolian Medicine Preparation Center, No. 20160909) groups: TFFC were ground into powder and prepared into CMC-Na suspension before being used for gavage for 14 consecutive days (150, 300, and 600 mg/kg/day, respectively). At 2 h after the completion of gavage on day 14, LAD was ligated for 1 min. Then, reperfusion was performed after resuming the blood stream. The positive control group: Compound Danshen Dripping Pill powder was suspended in CMC-Na and used for gavage for 14 days in a row (300 mg/kg/days). At 2 h after the completion of gavage on day 14, LAD was ligated for 1 min. Then, reperfusion was performed after resuming

798

Zhang et al. Anti-MIRI mechanism of TFFC

the blood stream.

Establishment of the MIRI model

After the Sprague-Dawley (SD) rats were preconditioned with TFFC for 2 weeks, 3% sodium pentobarbital (1 mL/kg) was intraperitoneally injected. After successfully administering anesthesia, these animals were placed in supine position to fix their extremities, treated with tracheal intubation and connected with small animal ventilators (tidal volume 20 mL/kg, respiratory quotient 1:2, frequency 40 times/min). The furs on the chest were removed, and the skin of left chest was disinfected with 75% alcohol. Pin electrodes of small animal electrocardiograph (ECG) were inserted subcutaneously into the four extremities before operation. Dynamic ECG was also monitored. Thoracotomy was performed at the left 3rd to 5th intercostal space (the site with the strongest heartbeat) along with the left midclavicular line. The chest skin was longitudinally cut off at approximately 2 cm. The muscle layer was dissected bluntly, and the pericardium was fully torn open to expose the heart. The great cardiac vein accompanying the left coronary artery was identified between the left auricle and arterial cone, and LAD was ligated with 5-0# ligature with the slipknot of 2 mm below the left auricle. Blocking was sustained for 60 s, depending on the ischemia severity. The combination of the T-wave change in ECG and myocardium at the corresponding site turning from to light red suggested the successful model establishment of myocardial ischemia. The ligature was released to resume the blood flow again. The heart was sent back to the chest quickly, and the chest was closed layer by layer after discharging the air and blood within the chest. A ventilator was disconnected to restore the autonomous respiration. The whole process proceeded by aseptic technique. ECG was recoded for all the model rats before and after model establishment and at different time points after scanning.

1[3N]-ammonia micro-PET/CT myocardial imaging

All animals were free to eat before imaging. The model rats were placed into a constant temperature anesthesia cabin. After being successfully anesthetized with 2.5% isoflurane mixed gas (V/V, isoflurane: oxygen), the model rats were placed on a micro-PET/CT (Innovation Drive MM, SIEMENS company) examination bed and fixed in supine position. Isoflurane mixed gas (3.5%, V/V, isoflurane: O) was used for sustained anesthesia. CT images were acquired, and 0.2 mL of 2 mci ^{13}N-ammonia was intravenously

injected into the tail of each rat. PET image was collected immediately 5 min after injection. The following are the parameters of CT image acquisition: voltage, 80 kV, current, 500 µÅ; slice thickness, 0.06 mm; number of slices, axial × coronal × sagittal =736×512×512; exposure time, 600 ms; and method of image reconstruction, Feldkamp. The parameters of PET image acquisition are as follows: time of acquisition: 10 min and field of view (FOV): 12.7 mm. The acquired images were processed by attenuation and correction. Feldkamp method is applied to image reconstruction. CT and PET images are obtained by SIEMENS Inveon MM workstation, and their fusion images are obtained.

Data processing and image interpretation

After completing image acquisition, the images were interpreted, calculated, and analyzed using SIEMENS Inveon MM IRW image fusion software. The micro-PET/CT images were reconstructed by Feldkamp algorithm to draw the myocardium as the region of interest (ROI). The mean standard uptake value of myocardial radioactive substance (SUV_{mean}) and volume of interest (VOI) were calculated after modeling. The images were read independently by two experienced nuclear medicine specialists by blind method. Any inconsistency between the two specialists in terms of diagnostic opinion would be decided through discussion.

Serological test

After myocardial ischemia/reperfusion, 5 mL of blood was collected from the Abdominal aorta of the rats and added with heparin before being centrifuged at 1,500 r·min^{-1} for 10 min. The serum was collected after finishing centrifugation. The serum LDH, CK, SOD, and MDA were determined by a fully automatic biochemical analyzer.

Observation of myocardial pathological structure

All model rats were sacrificed after completing imaging. Myocardial pathological observation was carried out by staining cardiac tissue with hematoxylin and eosin (HE). The isolated heart was washed with a fixative. The myocardial tissue on the left ventricular anterior wall was cut into strips and placed in a fixative for 2 h, then rinsed with 0.09 mmol KH_2PO_4 for 15 min, and stored in this solution. Conventional progressive dehydration in alcohol, transparency in xylene, conventional paraffin embedding, and intermittent uniform slicing were performed in order. After HE staining, the change in myocardial pathological

structure was observed under an optical microscope.

In vitro MIRI model investigation

Primary culture of neonatal rat myocardial cells

One to 3-day-old Wistar rats were disinfected with 75% alcohol and placed on a super clean bench. Ophthalmic scissors were inserted below the xiphoid process to cut the pleura and ribs upwards to expose the heart by gentle squeezing and cutting the myocardial tissue fully. This tissue was rinsed two times in low-temperature D-Hanks solution containing double antibody. The residual blood was washed to clean up the blood stains. The cleaned myocardial tissue was placed into a low-constant temperature flat dish and added with a small amount of D-Hanks solution. The myocardial tissue was cut into 1 mm^3 fragments with another pair of disinfected ophthalmic scissors. These fragments were transferred to a small conical flask by a long-head pipette. A total of 5 mL of trypsin-EDTA solution were added into a 50 mL flask and blown by a rubber head pipette repeatedly to allow the myocardial fragments to contact with the digestive solution thoroughly. Then, the solution was shaken in water bath for 4 min at 37 °C. The procedures mentioned above were repeated two times before standing. After the tissue deposited, the supernatant was sucked up and abandoned. The red blood cells were eliminated as many as possible by washing in D-Hanks solution. A total of 5 mL of trypsin-EDTA solution were added into the flask to repeat the previous step. Digestion lasted for 10 min in a water bath shaker at 37 °C. After natural sedimentation, the supernatant was transferred to 1# 15 mL sterile centrifuge tube, and 15% fetal bovine serum (FBS) containing dulbecco's modified eagle medium (DMEM) precooled at 4 °C was added before being blown by a rubber head pipette repeatedly. The remaining deposited tissue was digested two times by the same method. After sucking up the supernatant, the remaining deposited tissue was transferred to 1# and 2# 15 mL sterile centrifuge tubes, respectively. When myocardial cells were separated and purified, the cell suspension was transferred to a 30 mL clean flask. The FBS concentration in DMEM was adjusted to 10%, 5-BrdU (0.1 mM/L) was added, the cell suspension was diluted by DMEM, and the number of cells was counted. The cell density of the suspension was adjusted to 1×10^4 cells/mL and inoculated to a multiwell plate. After heating on flame, the plate was sealed with a cover and placed into an incubator at 5% CO_2. The culture solution was changed after 12 h of incubation and changed to serum-free DMEM culture solution. The culture solution was changed once every 2 days.

MIRI myocardial cell model establishment

Myocardial cells cultured for 72 h were removed from the culture medium and washed with phosphate-buffered saline (PBS) solution once to two times, followed by introducing PBS solution incubated at 37 °C. The culture dish was placed into an anoxia box that was then filled with N_2 to create the required environment (5% CO_2, 95% N_2). The anoxia box was sealed and checked for gas leakage before being placed into an incubator for 3 h of culture at 37 °C. This method was used to build the anaerobic environment. The anoxia box was taken from the culture dish after 3 h before removing gently and replacing with the complete culture solution the PBS within the culture dish. Reoxygenation culture (5% CO_2 95% air, 37 °C) lasted for 3 h in a conventional culture box to complete the establishment of the MIRI myocardial cell model.

Experimental grouping

The experimental group consisted of six groups. The experimental operation was repeated for three to five times for each group.

Normal group: Considering the absence of other treatments, primary myocardial cells were cultured in normal oxygen environment.

Model group: After the culture solution was changed to anoxic solution, the primary myocardial cells were cultured in an anoxic device for 3 h. Next, the cells were cultured in normal oxygen environment after the solution was changed to reoxygenation culture solution.

Three dose groups: A total of 150 (low-dose group), 300 (medium-dose group), and 600 µg·mL^{-1} (high-dose group) TFFC were provided 24 and 1 h before anaerobic treatment. The myocardial cells were cultured for 3 h in an anoxic device after the culture solution was changed to anoxic solution. Then, the cells were cultured for 3 h in normal O environment after the culture solution was replaced with reoxygenation culture solution. Positive control groups: Compound Danshen Dripping Pills (300 µg·mL^{-1}) were given 24 and 1 h before the experiment. The primary myocardial cells were cultured under normal O.

Cells growing in good condition were digested with 0.25% trypsin. The cell density was adjusted to 2×10^5 cells/mL. These cells (primary myocardial cells) were inoculated to a 96-well plate. A total of 100 µL of cell suspension

800

Zhang et al. Anti-MIRI mechanism of TFFC

Table 1 Determining myocardial apoptosis by flow cytometry

Group	AnnexinV-FITC	PI
Negative control	–	–
Positive control	+	+
Single-positive 1	+	–
Single-negative 2	–	+

The single-positive and -negative tubes were arranged to adjust the light compensation of a flow cytometer and separate the cell groups.

were added into each well. After 24 h of culture (primary myocardial cells), it was changed to serum-free culture solution (2 mmol·L^{-1} Na$_2$S$_2$O$_4$) for further culture for 1 h. After the anoxic solution was discarded, the serum-free culture solution was used for further culture for 3 h. A total of 10 µL of CCK-8 solution were added into each well for culture at 37 ℃ for 1 h. Absorbance at 450 nm was determined by an ELISA instrument.

Morphological study of anoxia-induced myocardial injury

Primary cells: Prior to treatment, the myocardial cells in each group were observed under a reversed biological microscope to ensure that they were growing well. After the different experimental groups were given drug intervention, myocardial cells in the normal group grew in monolayer clusters and had many plump pseudopodia that beat in the same rhythm. Meanwhile, in the model group, intercellular spaces increased, and the number of cells decreased. Few pseudopodia, cell detachment, suspension, dissolution, necrosis, and other apparent injuries were also noted.

Hoechst staining

The cells growing in good status were digested with 0.25% trypsin. The cell density was adjusted to 2×10^5 cells/mL, and these cells were inoculated to a 24-well plate. Each well was added with 0.5 mL of cell suspension and 250 µL of Hoechst 33342 staining solution before incubation away from light for 30 min. After the staining solution was discarded, it was rinsed with PBS three times. Cell apoptosis was observed under a fluorescence microscope.

Determining myocardial apoptosis by flow cytometry

(I) The cells in good status were digested with 0.25% trypsin. After the cell density was adjusted to 6×10^5 cells/mL, these cells were inoculated into a 6-well plate. A total of

1 mL of cell suspension were added into each well. After taking out the 6-well plate, the culture solution of each well was sucked into a centrifuge tube. A total of 1 mL of enzyme (0.25% trypsin + 0.03%EDTA) were introduced to each well for digestion. After these cells were fully digested, the medium in the same volume was added to stop the digestion before being transferred to the corresponding 15 mL centrifuge tube for centrifugation for 5 min at 1,000 r/min. (II) The cells were resuspended with 5 mL of precooled PBS and centrifuged for 5 min at 1,000 r/min. (III) The cells were resuspended with 1 mL of precooled PBS, and the cell solution was transferred to the corresponding 15 mL centrifuge tube for centrifugation for 5 min at 1,000 r/min. After PBS was discarded, the solution was resuspended with 100 µL of binding buffer. (IV) Four single-positive tubes were processed, as follows: a. single-positive tubes 1A and 2A (56 ℃, 7 min) and b. single-positive tubes 1B and 2B (56 ℃, 10 min). Other samples were double-stained (56 ℃, 5 min). (V) Each tube was added with 100 µL of cell suspension. A total of 5 µL of corresponding dye were added as follows (*Table 1*).

Statistical analysis

All the data obtained were analyzed using SPSS22.0 software, and significant level α was set at P=0.05. Quantitative data satisfying normal distribution and homogeneity of variance were expressed as mean ± standard deviation ($\overline{x} \pm s$) to describe the data indicators statistically. Quantitative data failing to satisfy the normal distribution or homogeneity of variance were expressed as median ± interquartile range to describe the data indicators statistically. Variance analysis was carried out for comparison in and between groups. Paired t-test was conducted on paired datasets. P<0.05 was considered statistically significant.
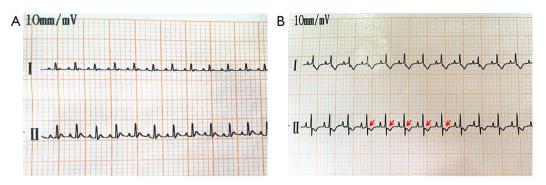
All experiments were approved by the Animal Care and Use Committee of Inner Mongolia Medical University (Hohhot, Inner Mongolia) (NO. YKD2017092) and were in accordance with Guide for Care and Use of Laboratory Animals (National Institutes of Health, Bethesda, MD, USA).
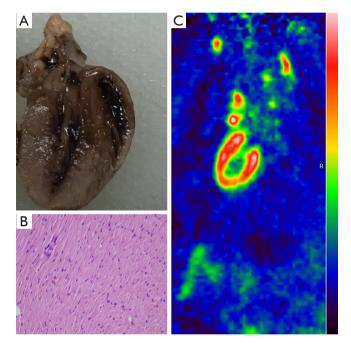
Results

In vivo MIRI model investigation

Establishment of myocardial ischemia/reperfusion model

A total of 120 SD rats were blocked at the anterior inferior

Figure 1 ECG of normal and myocardial ischemia model of rats. (A) ECG of normal rats before modeling. (B) ECG of myocardial ischemia model of rats (lead II T-wave change with >0.2 mV depression in ST segment in ECG after modeling suggested successful establishment of myocardial ischemia rat model, as indicated by the red arrow).

Figure 2 Gross anatomy of normal myocardial tissue. (A) Gross anatomy of normal myocardial tissue. (B) Pathology of normal myocardial tissue. (C) Perfusion imaging of normal myocardial tissue. Uniform ^{13}N-ammonia uptake in each wall of the left ventricle.

1/3 segment of the left anterior descending coronary artery. Among these rates, nine died during modeling (i.e., two in the low-dose group, one in the medium-dose group, three in the high-dose group, one in the model control group, and three in the positive control group). Four rats died

of anesthetic accident (1 in the low-dose group, 1 in the medium-dose group, 1 in the positive control group, and 1 in the model control group). Five rats died during imaging (1 in the blank control group, 2 in the low-dose group, 1 in the medium-dosage group, and 1 in the positive control group). The remaining 102 rats had lead II T-wave change with >0.2 mV depression in the ST segment in ECG. This result indicated successful modeling (*Figure 1A,B*). The comparisons between the blank control and model control groups in histopathology and molecular imaging are as follows (*Figure 2,3*).

Changes in VOI and SUV$_{mean}$ of *in vivo* MIRI model following dosing

The images were analyzed using SIEMENS Inveon MM IRW image infusion software to calculate the VOI. *Table 2* and *Figures 4,5,6,7,8A* show the VOIs of the low-, medium-, and high-dosage TFFC groups. Low-, medium-, and high-dose TFFC can protect the myocardium. High-dose group achieved the best effect. *Table 3* and *Figure 8B* show the SUV$_{mean}$ at the site of myocardial ischemia of the low-, medium-, and high-dose groups at each time point. The SUV$_{mean}$ value at the site of myocardial ischemia increased with time, and metabolism was gradually recovered, thereby suggesting that low-, medium-, and high-dose TFFC can protect the impaired myocardium. High-dose group achieved the best effect.

Test results of biochemical indicators.

The levels of serum oxidative stress indicators (i.e., SOD and MDA) and the activities of myocardial enzymes (CK
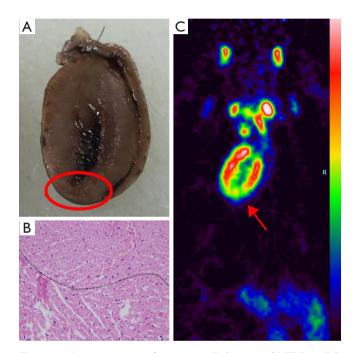
802

Zhang et al. Anti-MIRI mechanism of TFFC

and LDH) of rats in each experimental group are shown in *Table 4* and *Figure 9*.

In vitro MIRI model investigation

Morphological study of anoxia-induced myocardial injury under influence of TFFC

Following drug intervention, different experimental groups were observed under a reversed optical microscope. Myocardial cells in the normal group grew in monolayer

clusters and had many plump pseudopodia that beat in the same rhythm. Meanwhile, in the MIRI model group, intercellular spaces increased, and the number of cells decreased. Few vacuoles in the cytoplasm and pseudopodia were also observed. Cell detachment, suspension, dissolution, necrosis, and other evident injuries were observed. Compared with the MIRI model group, the morphology of the myocardial cells was improved to varying degrees in the low-, medium-, and high-dose groups. The high-dose group achieved the best effect. The results are shown in *Figure 10*.

Observation on morphology of myocardial cell apoptosis by Hoechst staining
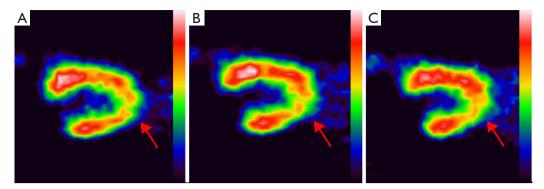
Hoechst fluorescence nuclear staining showed that myocardial cells in the normal control group were uniform with hyperchromatic nuclei and had no abnormal nuclei, as shown in *Figure 11A*. The cells in the model group were in typical apoptosis, and chromatin concentration, karyopyknosis, karyorrhexis, a small number of cells and many morphological characteristics of apoptosis were observed under a microscope, as shown in *Figure 11B*. Karyopyknosis, karyorrhexis, and other phenomena significantly decreased, and the number of cells was increased in a dose-dependent manner (*Figure 11C,D,E,F*).

Apoptosis rate of myocardial cells detected by flow cytometer

Compared with the normal control group (*Figure 12A*), the apoptosis rate of myocardial cells in the model group significantly increased (*Figure 12B*). Compared with the model group, the apoptosis rates of myocardial cells in the low-dosage TFFC, medium-dosage TFFC, high-dosage TFFC, and positive control groups significantly decreased (*Figure 12C,D,E,F*). The apoptosis rates were statistically analyzed, thereby suggesting that TFFC can evidently

Figure 3 Gross anatomy of rat myocardial tissue of MIRI model. (A) Gross anatomy of the MIRI myocardial tissue. (B) Pathology of the MIRI myocardial tissue (HE staining, ×400). (C) Perfusion imaging of MIRI myocardial tissue. Sparse ^{13}N-ammonia uptake at the left ventricular apex.

Table 2 Comparisons of VOI (mm^3) of various doses TFFC at different time points (N=102)

Group	24 h	48 h	72 h	F	P
Blank control (n=19)	–	–	–	–	–
Model control (n=18)	7.13±2.42	7.02±1.84	6.98±2.18	0.041	0.960
Low dose (n=15)	6.33±2.02	3.31±1.33	1.26±0.68	46.52	0.001
Medium dose (n=17)	6.01±1.56	2.61±1.01	0.00±0.00	110.71	0.000
High dose (n=17)	3.32±0.86	1.32±0.58	0.00±0.00	116.72	0.000
Positive control (n=16)	4.12±0.69	2.38±0.90	0.00±0.00	150.33	0.000

Figure 4 Perfusion imaging of MIRI model control group at different time periods. Control group: (A) 24 h, (B) 48 h, and (C) 72 h. As shown by the red arrow, the sparse area of imaging agent uptake at the left ventricular apex displayed insignificant change with time.
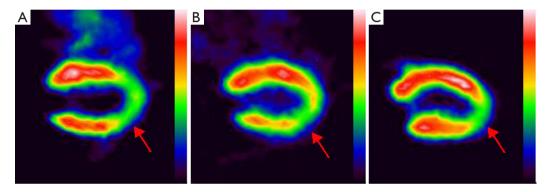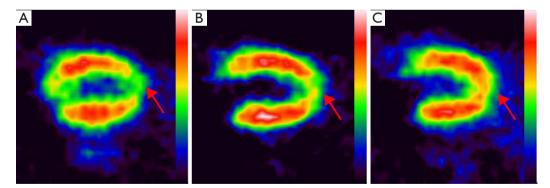

Figure 5 VOI image of low-dose group. Low-dose group: (A) 24, (B) 48, and (C) 72 h. As shown by the red arrow, the sparse area of imaging agent uptake at the left ventricular apex gradually decreases with time.

Figure 6 VOI image of medium-dose group. Medium-dose group: (A) 24, (B) 48, and (C) 72 h. As shown by the red arrow, the sparse area of imaging agent uptake at the left ventricular apex gradually decreases and even disappears with time.
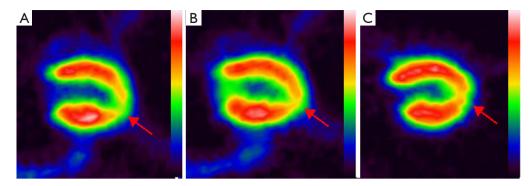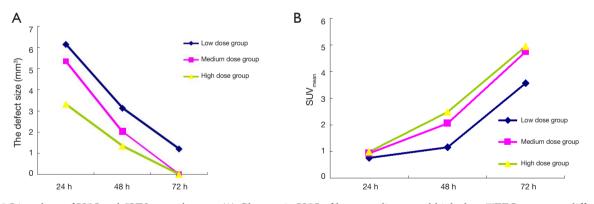
804

Zhang et al. Anti-MIRI mechanism of TFFC

Figure 7 VOI image of high-dose group. High-dose group: (A) 24, (B) 48, and (C) 72 h. As shown by the red arrow, the sparse area of imaging agent uptake at the left ventricular apex gradually decreases and even disappears with time.

Table 3 Comparisons of SUV_{mean} at the site of myocardial ischemia of various doses TFFC at different time points (N=102)

Group	24 h	48 h	72 h	F	P
Blank control (n=19)	4.98±0.48	5.05±0.47	5.04±0.42	0.095	0.910
Model control (n=18)	0.61±0.21	0.71±0.18	0.75±0.17	2.408	0.102
Low dose (n=15)	0.77±0.16	1.22±0.52	3.62±0.76	121.82	0.000
Medium dose (n=17)	0.94±0.15	2.11±0.50	4.75±0.33	450.82	0.000
High dose (n=17)	0.97±0.16	2.45±0.44	4.94±0.44	435.75	0.000
Positive control (n=16)	0.95±0.14	2.40±0.40	4.81±0.35	556.83	0.000

Figure 8 Line chart of VOI and SUVmean changes. (A) Changes in VOI of low-, medium-, and high-dose TFFC groups at different time points. (B) Changes in SUV_{mean} at site of myocardial ischemia of low-, medium-, and high-dose TFFC groups at different time points.
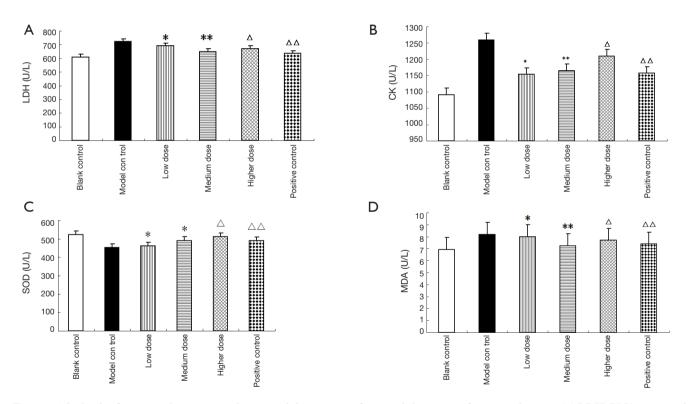
inhibit myocardial apoptosis.

Discussion

MIRI is mainly associated with inflammatory response, blood flow disturbance, endothelial cell injury, myocardial cell necrosis and apoptosis (11). MIRI can cause cardiac dysfunction, abnormal biochemical metabolism, enlarged myocardial infarction size, and pathological change in the myocardial tissue. MIRI is one of the important causes of secondary cardiac failure and cardiac death. O-free radicals mainly include O_{-2}, H_2O_2, and OH. These O radicals, especially OH, react with almost all organic matters within cells and destroy the nucleic acids, proteins,
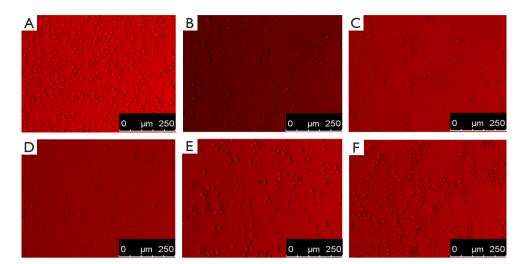
Table 4 The levels of serum SOD, MDA, CK and LDH of rats in each experimental group (N=102)

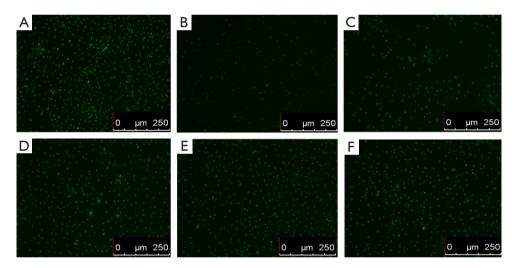| Group	Dose (mg/kg)	LDH (U/L)	CK (U/L)	SOD (U/mL)	MDA (nmol/g)
Blank control (n=19)	–	609.54±142.41	1091.45±195.141	523.51±27.65	6.91±1.42
Model control (n=18)	–	721.51±138.53	1259.37±207.17	452.45±30.17	8.17±1.93
Low dose (n=15)	150	691.73±162.27*	1153.74±187.81*	462.82±37.14*	7.98±1.26*
Medium dose (n=17)	300	649.92±171.25**	1165.42±167.83**	491.38±24.19**	7.24±1.08**
High dose (n=17)	600	671.38±168.69$^{\triangle}$	1209.84±163.47$^{\triangle}$	511.83±23.86$^{\triangle}$	7.69±1.34$^{\triangle}$
Positive control (n=16)	300	636.28±151.6$^{\triangle\triangle}$	1157.42±148.43$^{\triangle\triangle}$	490.87±27.72$^{\triangle\triangle}$	7.38±1.26$^{\triangle\triangle}$

LDH (U/L): compared with blank control group, *F=21.04, P=0.001, **F=20.78, P=0.001, $^{\triangle}$F=18.12, P=0.001, $^{\triangle\triangle}$F=19.22, P=0.001; compared with model control group, *F=6.95, P=0.002, **F=4.64, P=0.015, $^{\triangle}$F=4.58, P=0.016, $^{\triangle\triangle}$F=3.53, P=0.035. CK (U/L): compared with blank control group, *F=24.04, P=0.001, **F=23.78, P=0.001, $^{\triangle}$F=26.34, P=0.001, $^{\triangle\triangle}$F=23.78, P=0.001; compared with model control group, *F=7.12, P=0.001, **F=6.89, P=0.001, $^{\triangle}$F=7.22, P=0.001, $^{\triangle\triangle}$F=7.38, P=0.001. SOD (U/mL): compared with blank control group, *F=25.07, P=0.001, **F=24.33, P=0.001, $^{\triangle}$F=25.39, P=0.001, $^{\triangle\triangle}$F=24.79, P=0.001; compared with model control group, *F=7.13, P=0.001, **F=6.99, P=0.001, $^{\triangle}$F=7.12, P=0.001, $^{\triangle\triangle}$F=6.99, P=0.001. MDA (nmol/g): compared with blank control group, *F=4.17, P=0.022, **F=4.58, P=0.016, $^{\triangle}$F=3.81, P=0.030, $^{\triangle\triangle}$F=4.48, P=0.017; compared with model control group, *F=4.69, P=0.014, **F=3.97, P=0.026, $^{\triangle}$F=7.25, P=0.001, $^{\triangle\triangle}$F=6.65, P=0.001.

Figure 9 The levels of serum oxidative stress indicators and the activities of myocardial enzymes of rats in each group. (A) LDH (U/L): compared with blank control group, *F=21.04, P=0.001, **F=20.78, P=0.001, $^{\triangle}$F=18.12, P=0.001, $^{\triangle\triangle}$F=19.22, P=0.001; compared with model control group, *F=6.95, P=0.002, **F=4.64, P=0.015, $^{\triangle}$F=4.58, P=0.016, $^{\triangle\triangle}$F=3.53, P=0.035. (B) CK (U/L): compared with blank control group, *F=24.04, P=0.001, **F=23.78, P=0.001, $^{\triangle}$F=26.34, P=0.001, $^{\triangle\triangle}$F=23.78, P=0.001; compared with model control group, *F=7.12, P=0.001, **F=6.89, P=0.001, $^{\triangle}$F=7.22, P=0.001, $^{\triangle\triangle}$F=7.38, P=0.001. (C) SOD (U/mL): compared with blank control group, *F=25.07, P=0.001, **F=24.33, P=0.001, $^{\triangle}$F=25.39, P=0.001, $^{\triangle\triangle}$F=24.79, P=0.001; compared with model control group, *F=7.13, P=0.001, **F=6.99, P=0.001, $^{\triangle}$F=7.12, P=0.001, $^{\triangle\triangle}$F=6.99, P=0.001. (D) MDA (nmol/g): compared with blank control group, *F=4.17, P=0.022, **F=4.58, P=0.016, $^{\triangle}$F=3.81, P=0.030, $^{\triangle\triangle}$F=4.48, P=0.017; compared with model control group, *F=4.69, P=0.014, **F=3.97, P=0.026, $^{\triangle}$F=7.25, P=0.001, $^{\triangle\triangle}$F=6.65, P=0.001.
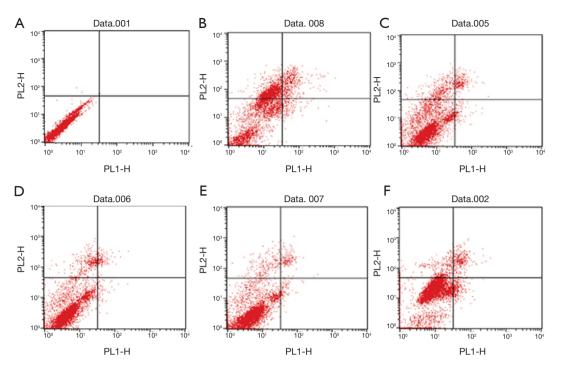
Figure 10 Morphological study of anoxia-induced myocardial injury under influence of TFFC. (A) Normal group, (B) model group, (C) low-dose group, (D) medium-dose group, (E) high-dose group, and (F) positive control group.

Figure 11 Morphology of myocardial cell apoptosis by Hoechst staining. (A) Normal group, (B) model group, (C) low-dose group, (D) medium-dose group, (E) high-dose group, and (F) positive control group.

amino acids, and lipid compounds, thereby damaging the cell function (5). In normal physiological conditions, antioxidants within cells can eliminate O-free radicals in time. Hence, free radical generation and degradation maintain dynamical equilibrium. However, after the blood and O supplies are restored following myocardial ischemia/reperfusion, a considerable amount of O-free radicals would be generated and accumulated rapidly. The production of free radicals far exceeds the scavenging capacity of the endogenous antioxidant system, which triggered chain lipid peroxidation reaction (12), damaged the cell membrane, organelle, and even nucleic acid; and caused intracellular

Ca overload decreased. This condition led to acute or chronic myocardial injury and resulted in cell necrosis and apoptosis.

[13]N-ammonia PET imaging can evaluate the degree and dynamic development of myocardial perfusion injury in early stage. Some researchers (13,14) used ^{13}N-ammonia PET imaging to qualitatively and quantitatively observe the changes of blood flow and function of Beagle dogs' heart after local radiotherapy, confirming that ^{13}N-ammonia PET can be used for early detection and detection of changes of cardiac injury. Our research shows that ^{13}N-ammonia PET blood perfusion of damaged myocardial blood in

Figure 12 Apoptosis rate of myocardial cells detected by flow cytometer. (A) Normal group, (B) model group, (C) low-dose group, (D) medium-dose group, (E) high-dose group, and (F) positive control group.

MIRI decreases, which may be due to endothelial cell injury, inflammatory reaction, microvascular injury caused by expression of inflammatory factors, myocardial hypoxia ischemia and interstitial fibrosis (15,16). All dose groups of TFFC have protective effects on MIRI, which can restore the blood perfusion of damaged myocardium and gradually increase SUV_{mean}. The high dose group has good effect.

At present, most of the methods to study the efficacy and pharmacodynamic mechanism of Mongolian medicine use serological detection, pharmacology, pharmaceutics or myocardial histopathology *in vitro* (17-19). We use molecular imaging methods combined with serology, histopathology, Hochest staining and flow cytometer detection to carry out comparative study on traditional Mongolian medicine. The results show that PET/CT molecular imaging method can detect the efficacy of TFFC against MIRI *in vivo* at an early stage, and this method is non-invasive and can dynamically observe myocardial perfusion changes after TFFC treatment in vivo.

Serum lactate dehydrogenase (LDH) and creatine kinase (CK) levels are considered as markers of myocardial injury. After myocardial ischemia-reperfusion occurs, CK is released in a large amount, resulting in obvious

enhancement of CK activity in serum (20). Compared with CK, although LDH activity appears later, it lasts for a long time, and the degree of activity increase is closely related to the degree of myocardial injury. The larger the injury range, the higher the LDH activity. Superoxide dismutase (SOD) is a free radical scavenger, which widely exists in various tissues of organisms, can scavenge free radical O_2 (superoxide anion radical) and catalyze the disproportionation reaction of free radicals in organisms. Malondialdehyde (MDA) content is an indicator of peroxidation, which can indirectly reveal the level of ROS generation and is a marker to measure oxidative stress response. Our research confirmed that three dosage groups of TFFC can remove free radicals *in vivo* and protect myocardium from ischemia-reperfusion injury, of which the high dosage group has the best effect on SOD, and the SOD content increases to 511.83±23.86 $U·mL^{-1}$ after administration, which is close to the normal level. The middle dose group had the best effect on MDA, and the content of MDA decreased to 7.24±1.08 $nmol·g^{-1}$, close to the normal level (P<0.05). The low dose group had the best effect on CK, and the content of CK decreased to 1,153.74±187.81 $U·L^{-1}$, close to the normal level. However, the medium dose group had the best effect on

808

Zhang et al. Anti-MIRI mechanism of TFFC

LDH. After administration, the LDH content decreased to 649.92 ± 171.25 $U\cdot L^{-1}$, close to the normal level.

Oxidative stress is one of the important causes of cell apoptosis, and its effect on aging has been continuously recognized in recent years (21). Harman proposed the free radical theory of aging. He believed that aging is caused by two mechanisms, one is the action of intracellular peroxides, which causes oxidative stress reaction of cells and aging, and the other is mitochondrial respiration (22). Oxidative stress can induce apoptosis (23,24) by regulating apoptosis gene-related pathways. Our research proves that TFFC can inhibit myocardial cell apoptosis and reduce myocardial cell apoptosis rate.

Furthermore, previous literatures report that myocardial blood flow is decreased locally in human and dog following ischemia reperfusion after at least 15min of coronary occlusion (25,26). However, there are controversies over the duration of coronary occlusion in the model of acute myocardial ischemia in rats, or relevant studies are rarely seen.

Before this experiment, we determined the time widow of acute myocardial ischemia (AMI): 50 SD rats were selected and randomly divided into five groups according to time of coronary occlusion: 15, 10, 5, 2 and 1 min group. ^{13}N-ammonia Micro PET/CT myocardial perfusion imaging was performed 2, 24 and 48 h after ischemia-reperfusion. 6 model rats died during modeling, 5 died during imaging, and a total of 39 rats complete all the imaging. Among them, 30 model rats (6 in 15 min group, 7 in 10 min group, 9 in 5min group and 8 in 2 min group) presented sparse or defect areas in 48 h 13N-ammonia myocardial perfusion imaging, and lead II Q-wave appeared in ECG, indicating myocardial infraction. 9 model rats (in 1min group) recovered normal in 48 h ^{13}N-ammonia imaging. Therefore, time of coronary artery ligation for AMI was finalized as 1min, which is slightly different from other related reports (27,28). This would be further explored and verified in our subsequent studies.

Conclusions

We used molecular imaging combined with other detection methods to study the mechanism of traditional Mongolian medicine, confirmed that the anti-MIRI of TFFC can scavenge free radicals, reduce oxidative stress damage, inhibit apoptosis, affect the activity of related enzymes and so on. ^{13}N-ammonia PET/CT Myocardial Imaging can

noninvasively evaluate the anti-MIRI effect of TFFC *in vivo* by observing the dynamic changes of blood perfusion of damaged myocardium at an early stage, providing a new diagnostic method and research idea for the development of traditional Mongolian medicine in the future.

Footnote

Reporting Checklist: The authors have completed the ARRIVE reporting checklist. Available at http://dx.doi.org/10.21037/cdt-20-305

Data Sharing Statement: Available at http://dx.doi.org/10.21037/cdt-20-305

Conflicts of Interest: All authors have completed the ICMJE uniform disclosure form (available at http://dx.doi.org/10.21037/cdt-20-305). The authors have no conflicts of interest to declare.

Ethical Statement: The authors are accountable for all aspects of the work in ensuring that questions related to the accuracy or integrity of any part of the work are appropriately investigated and resolved. All experiments were approved by the Animal Care and Use Committee of Inner Mongolia Medical University (Hohhot, Inner Mongolia) (NO. YKD2017092) and were in accordance with Guide for Care and Use of Laboratory Animals (National Institutes of Health, Bethesda, MD, USA).

Open Access Statement: This is an Open Access article distributed in accordance with the Creative Commons Attribution-NonCommercial-NoDerivs 4.0 International License (CC BY-NC-ND 4.0), which permits the non-commercial replication and distribution of the article with the strict proviso that no changes or edits are made and the original work is properly cited (including links to both the

formal publication through the relevant DOI and the license). See: https://creativecommons.org/licenses/by-nc-nd/4.0/.

References

1. Chen WW, Gao RL, Liu LS, et al. Summary of china cardiovascular disease report 2017. Chinese Circulation Journal 2018;33:1-8.

2. Heusch G, Gersh BJ. The pathophysiology of acute myocardial infarction and strategies of protection beyond reperfusion: a continual challenge. Eur Heart J 2017;38:774-84.

3. Jennings RB, Sommers HM, Herdson PB, et al. Ischemic injury of myocardium. Ann N Y Acad Sci 1969;156:61-78.

4. Yang S, Yang C, Tian Y, et al. Protective effect of fistular onion bulb extract on myocardial ischemia/reperfusion injury. Acta Anatomica Sinica 2020;51:258-64.

5. Han BBL. Clinical observation on 55 cases of stable angina pectoris treated with mongolian medicine Guangzao Qiwei powder. Chinese Journal of Ethnomedicine and Ethnopharmacy 2010;19:8.

6. Na RMDL, Se TY, Zhao RGT. Experience of mongolian medicine Guangzao Qiwei pill in the treatment of coronary heart disease. Journal of Medicine & Pharmacy of Chinese Minorities 2004;10:30.

7. Wu H, Yang Y. Research status of Mongolian pharmacology. Chinese Journal of Ethnic Medicine 2012;18:45-8.

8. Zhao D, Wang R, He J, et al. Comparative experiments on extraction and content determination of flavonoids in jujube leaves and jujube, Journal of Baotou Medical College 2019;35:70-2.

9. Bao L, Zhou L, Huang Z. Research about Mongolian medicine myristica fragranr houtt-5. China Medicine and Pharmacy 2012;2:57-63.

10. Liu T, Zhu D, Shu L, et al. Effects of total flavonoids of Canton jujube on angiotensin II induced myocardial fibrosis in rats. Chinese Journal of Ethnic Medicine 2014;12:55-8.

11. Bromage DI, Taferner S, He Z, et al. Stromal cell-derived factor-1αsignals via the endothelium to protect the heart against ischaemia-reperfusion injury. J Mol Cell Cardiol 2019;128:187-97.

12. Liu PK, Grossman RG, Hsu CY, et al. Ischemic injury and faulty gene transcripts in the brain. Trends Neurosci 2001;24:581-8.

13. Zhu J, Song J, Yan R, et al. Dynamic changes in blood flow and function of the heart using 13N-NH3 PET gated myocardial perfusion imaging in Beagle dogs after local heart irradiation. Chinese Journal of Nuclear Medicine and Molecular Imaging 2018;38:471-5.

14. Song J, Yan R, Wu z, et al. 13N-Ammonia PET/CT detection of myocardial perfusion abnormalities in Beagle dogs after local heart irradiation. J Nucl Med 2017;58:605-10.

15. Boerma M. Experimental radiation-induced heart disease: past, present, and future. Radiat Res 2012;178:1-6.

16. Taunk NK, Haffty BG, Kostis JB, et a1. Radiation-induced heart disease: pathologic abnomalities and putative mechanisms. Front Oncol 2015;5:39.

17. Gao W, Yu M, Xiao Y, et al. Pharmacokinetic Analysis of Nutmeg Bawei Powder. China Journal of Experimental Traditional Medical Formulae 2016;22:82-5.

18. Zhang YY, Xiao YF, Li WY, et al. Effects of roudoukou-8 san extract on hydrogen peroxide induced cardiomyocyte injury. Medicinal Plant 2018;9:101-10.

19. Xiao Y, Li W, Wang Y. Study on the Protective Effects of Mongolian Medicine Roudoukou-8 Powder on Cardiac Tissue of Experimental Animals. China Pharmacy 2018;29:2944-8.

20. Yin J, Yang R, Zhao X, et al. Study on Protective Effect of Total Flavonoids from the Leaves of Mongolian Medicine Choerospondias axillaris on Myocardial Ischemia Reperfusion Injury Model Rats. China Pharmacy 2019;30:2253-7.

21. Yu JM, Zhang XB, Jiang W, et al. Astragalosides promote angiogenesis via vascular endothelial growth factor and basic fibroblast growth factor in a rat model of myocardial infarction. Mol Med Rep 2015;12:6718-26.

22. Harman D. The free radical theory of aging. Antioxid Redox Signal 2003;5:557-61.

23. Kwok SS, Bu Y, Lo AC, et al. A systematic review of potential therapeutic use of lycium barbarum polysaccharides in disease. Biomed Res Int 2019;2019:4615745.

24. Severino P, D'Amato A, Netti L, et al. Myocardial ischemia and diabetes mellitus: role of oxidative stress in the connection between cardiac metabolism and coronary blood flow. J Diabetes Res 2019;2019:9489826.

25. Rashba EJ, Lamas GA, Couderc JP, et al. Electrophysiological effects of late percutaneous coronary intervention for infarct-related coronary artery occlusion: the Occluded Artery Trial-Electrophysiological Mechanisms (OAT-EP). Circulation 2009;119:779-87.

26. Ravingerova T, Neckar J, Kolar F, et al. Ventricular arrhythmias following coronary artery occlusion in rats: is

the diabetic heart less or more sensitive to ischaemia? Basic Res Cardiol 2001;96:160-8.

27. Gao H, Kiesewetter DO, Zhang X, et al. PET of glucagonlike peptide receptor upregulation after myocardial ischemia or reperfusion injury. J Nucl Med 2012;53:1960-8.

28. Thukkani AK, Shoghi KI, Zhou D, et al. PET imaging of in vivo caspase-3/7 activity following myocardial ischemia-reperfusion injury with the radiolabeled isatin sulfonamide analogue [(18)F]WC-4-116. Am J Nucl Med Mol Imaging 2016;6:110-9.